

Manufacture and Characterization of Cationic Nano-fibrillated Cellulose from Cotton Pulp

Soo Hyun Lee,^a Hae Min Jo,^a and Ji Young Lee^{b,*}

The applicability of cotton-bleached soda pulp (C-BSP) was investigated as a raw material for manufacturing cationic nano-fibrillated cellulose (NFC) *via* quaternization of anionic NFC using glycidyl-trimethyl-ammonium chloride (GMA). The anionic NFC was prepared by beating and micro-grinding C-BSP, and quaternization was performed post treatment to induce a charge reversal in anionic NFC. The characteristics of cationic NFC manufactured using C-BSP and hardwood-bleached kraft pulp (Hw-BKP) as a control were analyzed. Relatively higher mechanical energy was required to prepare anionic NFC from C-BSP than that from Hw-BKP. Fourier transform infrared and zeta potential analyses results showed that quaternization by GMA post treatment electrostatically induced charge reversal in anionic NFC. However, GMA did not affect the fiber width and viscosity of the cationic NFCs. It was found that cationic NFC could be manufactured *via* quaternization of anionic NFC manufactured from C-BSP using less GMA than that for Hw-BKP.

DOI: 10.15376/biores.18.2.3328-3341

Keywords: Nano-fibrillated cellulose (NFC); Cotton bleached soda pulp; Quaternization; Glycidyl-trimethyl-ammonium chloride (GMA); Zeta-potential; Charge reversal

Contact information: a: Department of Forest Products, Gyeongsang National University, Jinju 52828, Republic of Korea; b: Department of Environmental Materials Science/IALS, Gyeongsang National University, Jinju 52828, Republic of Korea; *Corresponding author: paperyjy@gnu.ac.kr

INTRODUCTION

Nanocellulose, which is a biodegradable, non-toxic, and sustainable natural resource, can be defined as cellulose particles with a fibrillar width less than 100 nm (Nechporchuk *et al.* 2016; Candan *et al.* 2022). There are two main types of nanocellulose: nanocrystalline cellulose (NCC) and nano-fibrillated cellulose (NFC) (Balea *et al.* 2020; Naddeem *et al.* 2022). The ISO terms for these products are CNC and CNF, respectively.

NCC is commonly produced using the acid hydrolysis process using sulfuric acid. On the other hand, NFC can be manufactured through various mechanical treatments such as grinding, high-pressure homogenization, micro-fluidization, electrospinning, and steam explosion (Nechporchuk *et al.* 2016; Balea *et al.* 2020; Norizan *et al.* 2022). The NFC has been regarded as a promising material in many industries because of its low density, high aspect ratio, flexibility, and high mechanical strength (Eichhorn *et al.* 2010; Sato *et al.* 2016; Qin *et al.* 2020; Sanchez-Salvador *et al.* 2020).

Despite various studies on the functionalities and applications of NFC, NFC has not been industrialized worldwide, indicating that many issues need to be solved (Yi *et al.* 2020). These issues include high energy demand, low compatibility with other materials, lack of precise applications in various industries, and the need for new cellulose resources, not limited to woody resources (Ashori *et al.* 2014; Pennells *et al.* 2020; Yasim-Anuar *et al.* 2020; Candan *et al.* 2022). Because of the low self-sufficiency rate of woody resources in South Korea (Korea Rural Economics Institute 2020), novel cellulose resources should be developed for stable production and supply of NFC.

Cotton fiber, a seed fiber among non-woody fiber resources, is a natural cellulose fiber resource that can be grown quickly (Park and Kim 2010; Deng *et al.* 2022). Research has been underway to apply cotton fibers as industrial materials in Europe and China (Li *et al.* 2014; Ruiz-Caldas *et al.* 2022). When manufacturing NFC, cotton fiber is expected to have the advantage of high yield because of its relatively high alpha cellulose content and crystallinity (Sczostak 2009; Morais *et al.* 2013; Beltramino *et al.* 2018). Therefore, cotton fiber has been considered a non-woody fiber resource that could be effectively utilized for NFC manufacturing.

Most of the NFCs have generally been manufactured by combining various pre-treatments and mechanical treatments, which result in an anionic electrostatic charge of the NFC due to carboxylic acids (Aulin *et al.* 2010; Charreau *et al.* 2020; Zinge and Kandasubramanian 2020). The NFC with a negative charge has poor retention on the surfaces of other anionic materials used in papermaking during the paper forming process (Liimatainen *et al.* 2014). Therefore, developing a pre-treatment or post treatment technology that can change the electrostatic characteristics of NFC fabricated from various cellulose resources is necessary.

Many studies have reported that quaternization is a common reaction for manufacturing cationic NFC. Cationic NFC was internally added during the papermaking and remained in the anionic fibers to be used as a strength enhancer (Lee *et al.* 2021) and was combined with anionic NFC to improve gas barrier properties to be used as a coating agent. (Jo *et al.* 2022). It was also used as an adsorbent for removing Cr from contaminated water (Etale *et al.* 2021) or a filter for removing anionic ions (Jo *et al.* 2021).

Glycidyl-trimethyl-ammonium chloride (GMA), Girard's agent T., and 3-chloro-2-hydroxy-propyl trimethyl-ammonium chloride (CHPTAC) have been primarily used to introduce quaternary amine groups to NFC molecules (Chaker and Boufi 2015; Bansal *et al.* 2021; Etale *et al.* 2021). However, because these are organic solvents that are not easy to handle and toxic to human health (Correia *et al.* 2021), it is required to minimize the use of organic solvents for manufacturing eco-friendly cationic NFC.

This study developed a technology to manufacture cationic NFC from cotton-bleached soda pulp (C-BSP) *via* quaternization using a minimum amount of GMA. Most previous studies have performed quaternization as a pre-treatment for manufacturing cationic NFC (Liimatainen *et al.* 2014; Nechyporchuk *et al.* 2016). However, this study reversed the zeta potential of anionic NFC through a post-treatment. Anionic NFC was prepared through beating and micro-grinding C-BSP. Then, quaternization was carried out using various amounts of GMA to prepare cationic NFC. Finally, the fiber width, low-shear viscosity, and zeta potential of cationic NFCs were measured to determine the minimum quantity of GMA required for preparing cationic NFC from C-BSP.

EXPERIMENTAL

Materials

The C-BSP was supplied by KOMSCO Co., Ltd. (Daejeon, Republic of Korea). Hardwood-bleached kraft pulp (Hw-BKP) was supplied by Moorim Paper Co., Ltd. (Jinju, Republic of Korea), as shown in Fig. 1. The C-BSP consisted of 60% cotton linter and 40% cotton noil. Glycidyltrimethylammonium chloride (GMA, C₁₆H₁₄ClNO, 99.00%) and N, N-dimethylacetamide (DMAc, C₄H₉NO, 99.50%) were purchased from Sigma-Aldrich (St. Louis, MO, USA). Potassium hydroxide flakes (KOH, 93.00%), ethyl alcohol (C₂H₅OH, 95.00%), and n-hexane (C₆H₄, 86.18%) were provided by Daejung Chemicals (Republic of Korea).

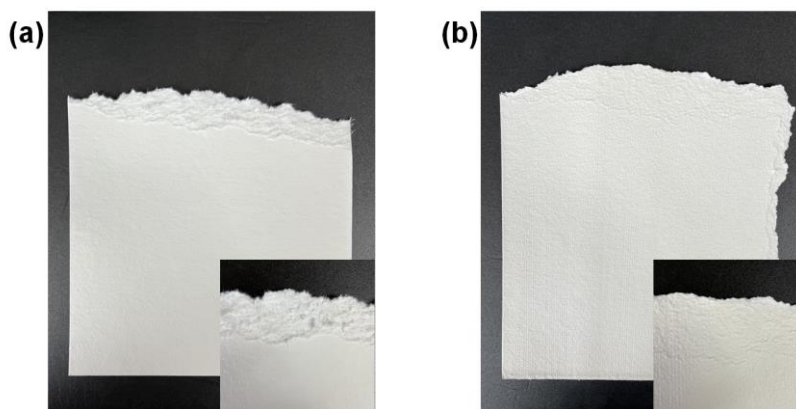


Fig. 1. Images of (a) C-BSP and (b) Hw-BKP

Methods

Chemical composition comparison between C-BSP and Hw-BKP

The chemical composition of Hw-BKP was analyzed as follows, and the extractive content and ash content were measured according to the following standards: KS M 7035 (2018) and TAPPI T211 om-07 (2007). The lignin content was analyzed using the chlorite method (Wise *et al.* 1946), and holocellulose was determined by weighing the delignified specimens, whereas alpha-cellulose was quantified by dissolving hemicellulose from delignified specimens using 17.5% NaOH. To compare the chemical composition of C-BSP with those of Hw-BKP, a reference search was carried out.

Preparation of anionic NFC from C-BSP and Hw-BKP

Anionic NFC was manufactured by beating and micro-grinding C-BSP as the sample and Hw-BKP as the control. The beating of C-BSP and Hw-BKP was performed at a consistency of 1.57% using a laboratory Hollander (valley) beater (FRANK-PTI GmbH, Birkenau, Germany). The C-BSP and Hw-BKP were beaten to a Canadian standard freeness (CSF) of 170 ± 5 and 450 ± 5 mL, respectively (Lee *et al.* 2017; Park *et al.* 2018). After beating the pulps, the fiber length and width of the beaten pulps were measured using a fiber analyzer (FQA-360; OpTest Equipment Inc., Hawkesbury, Canada). The beaten pulp was diluted to 1.0% consistency with distilled water and then fibrillated using a Super Mass Colloider (MKZA6-2, Masuko Sangyo Co., Ltd., Kawaguchi, Japan) at 1,500 rpm. The pulp slurry was fed continuously to the grinder consisting of two stone grinding disks

positioned on top of each other. The gap between the two disks was adjusted to about 150 μm . Four types of anionic NFC samples, manufactured from C-BSP and Hw-BKP, were taken at a micro-grinding pass number of five and seven (hereafter referred to as the pass number), respectively, as shown in Table 1.

Table 1. Manufacturing Conditions of anionic NFC from C-BSP and Hw-BKP

Pulp type	Pretreatment (Refining)	Mechanical treatment
C-BSP	170 mL CSF	Pass number = 5, 7
Hw-BKP	450 mL CSF	

Quaternization of anionic NFC to prepare cationic NFC

Cationic NFC was prepared from anionic NFC *via* quaternization of GMA (Chaker and Boufi 2015; Lee *et al.* 2019). The water was removed from the anionic NFC slurry using a centrifuge (LaboGene 1248, Gyrozen Co., Ltd., Republic of Korea), and solvent exchange was performed twice using DMAc. After NFC was conditioned at room temperature for 12 h, 10%, 20%, and 30% solutions of GMA and approximately 15 mL of 1.0 M KOH as a catalyst were added to the NFC. Afterwards, the quaternization was performed in a constant temperature water bath at 70 °C for 6 h, as shown in Table 2. The cationic NFC formed after the reaction was washed five times with 200-250 mL of distilled water and centrifuged to remove the remaining chemicals. Figure 2 shows the flow diagram for the quaternization of anionic NFC.

Table 2. Quaternization reaction condition for cationic NFC

Pulp Type of Anionic NFC	Dosage of KOH	Dosage of GMA	Temperature	Time
C-BSP	1.0 M 15 mL	10, 20, 30 (% on oven-dried fibers)	70 °C	6 h
Hw-BKP				

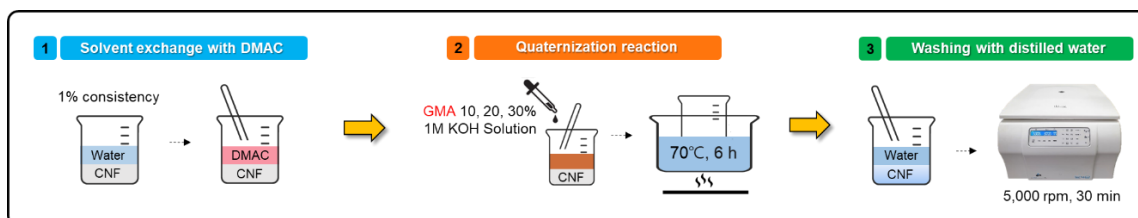


Fig. 2. Flow diagram of the quaternization of anionic NFC for preparing cationic NFC

Characterization of anionic and cationic NFCs

The fiber width and low-shear viscosity of NFCs were measured to evaluate their characteristics depending on the pulp type, the pass number of fibrillation, and the amount of GMA added. The fiber width of NFCs was analyzed using a field emission scanning electron microscope (FE-SEM; JSM-7610F, JEOL, Tokyo, Japan). Wet NFC pads were prepared as test specimens to measure the fiber width using a vacuum filtration system. The wet NFC pads were dried by the solvent exchange method using ethyl alcohol and n-

hexane to provide the dry test specimens (Oh *et al.* 2022). Afterward, the FE-SEM images of the pads were captured, and the fiber width was measured with image analysis using a three-dimensional (3D) image software (MP-45030TDI, JEOL, Osaka, Japan). The low-shear viscosity of 1.0% NFC slurries was determined using a low-shear viscometer (DV-IP, Brookfield Engineering Laboratories, Inc., Middleborough, MA, USA) with a spindle number of 64 and a speed of 60 rpm. The temperature of NFC slurries was maintained at 25 °C during the viscosity measurement.

Fourier-transform infrared (FT-IR) spectroscopy is a non-destructive technique to analyze the vibrations to detect functional groups in the molecular structure (Sofi *et al.* 2023). The spectra were used to determine the introduction of tertiary amino groups on a cationic NFC pad with a grammage of 100 g/m² using an FI-IR (IS50, Thermo Fisher Scientific, Waltham, MA, USA). To identify the modification of electrostatic properties of NFCs through a quaternization of GMA, the average zeta potential, and zeta potential distribution of 0.01% NFC slurries were measured using a Zeta-potential analyzer (Nano ZS, Malvern Panalytical, Malvern, UK).

RESULTS AND DISCUSSION

Chemical Composition Comparison between C-BSP and Hw-BKP

Table 3 shows the chemical composition of C-BSP reported in the previous study (Lee *et al.* 2022) and that of Hw-BKP measured in this study. The alpha-cellulose content of C-BSP was higher than that of Hw-BKP. The C-BSP had almost no hemicellulose content. The contents of other components in C-BSP did not show the significant difference from Hw-BKP. Therefore, C-BSP could have alpha-cellulose content sufficient for manufacturing NFC.

Table 3. Chemical Compositions of C-BSP and Hw-BKP

Chemical Composition (%)	Alpha-cellulose	Hemicellulose	Lignin	Extractives	Ash
C-BSP ^a	96.9	-	2.4	0.30	0.38
Hw-BKP ^b	80.8	18.0	1.2	0.04	0.01

^a cited from the literature (Lee *et al.* 2022) and ^b measured in laboratory

Fiber Width and Viscosity of NFC

In this study, anionic NFC was manufactured by beating and micro-grinding C-BSP and Hw-BKP. After that, cationic NFC was prepared *via* quaternization using GMA.

Figure 3 shows an image of cationic NFCs made from C-BSP and Hw-BKP at the pass number of seven by adding 30% of GMA to the oven-dried NFC fibers. Cationic NFCs made from C-BSP and Hw-BKP were visually not significantly different. Figure 4 shows the average fiber width of NFCs made from C-BSP and Hw-BKP as a function of added GMA amount and the micro-grinding pass number. Before adding GMA, the fiber width of anionic NFCs differed for C-BSP and Hw-BKP. When the pass number was five, most of the fibrils in C-BSP were more than 100 nm in diameter, which is a standard between

micro- and nano-fibrillated cellulose, and all the fibrils in Hw-BKP were nanosized. As the pass number increased from five to seven, all the fibrils in C-BSP and Hw-BKP were less than 100 nm. When comparing the two pulps, the fiber width of the anionic NFC made from Hw-BKP was lower than that of the anionic NFC made from C-BSP. This was because the fiber length and width of beaten Hw-BKP were lower than those of beaten C-BSP, as shown in Table 4. Thus, more mechanical treatment was required to manufacture anionic NFC using C-BSP than Hw-BKP. In contrast, the fiber length of NFCs from both pulps did not change considerably when the added amount of GMA was increased at the same pass number. Even though the pass number increased from five to seven, the fiber width of cationic NFC did not change noticeably with respect to the amount of GMA.

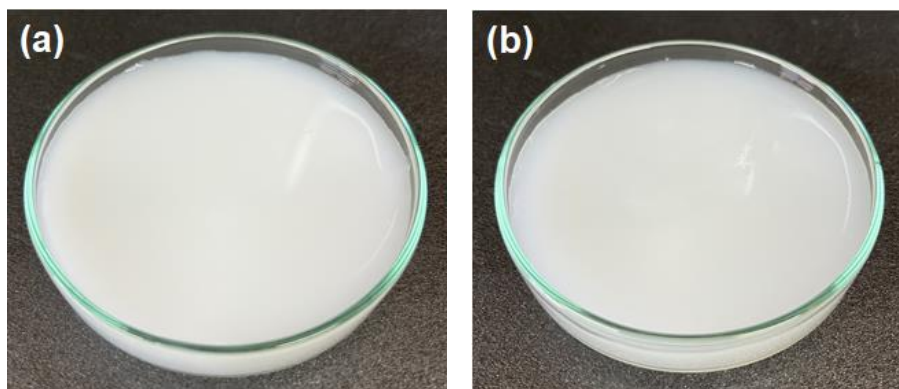


Fig. 3. Images of (a) NFCs manufactured from C-BSP and (b) NFCs manufactured from Hw-BKP NFCs at the pass number of seven by adding 30% of GMA to the oven-dried NFC fibers

Table 4. Average Fiber Length and Fiber Width of Beaten C-BSP and Hw-BKP before Micro-grinding

Pulp Type	C-BSP	Hw-BKP
Freeness	170 mL CSF	450 mL CSF
Average fiber length	1.0 mm	0.5 mm
Average fiber width	24.0 μm	18.4 μm

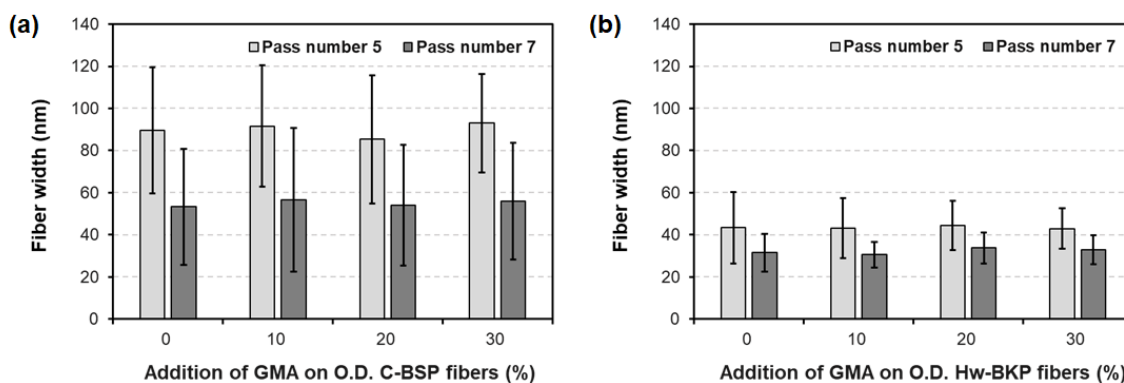


Fig. 4. Average fiber width of NFCs manufactured from (a) C-BSP and (b) Hw-BKP depending on the amount of GMA added and the pass number of micro-grinding

Figures 5 and 6 show the FE-SEM images of NFCs made from C-BSP and Hw-BKP, respectively, depending on the added amount of GMA at the pass number of seven. All the fibrils made from two pulps had a fiber width of less than 100 nm, indicating that the micro-grinding seven times was sufficient for manufacturing nanofibrils from C-BSP and Hw-BKP. These images also showed that the quaternization using GMA did not change the fiber width of the NFCs, which is consistent with Fig. 5.

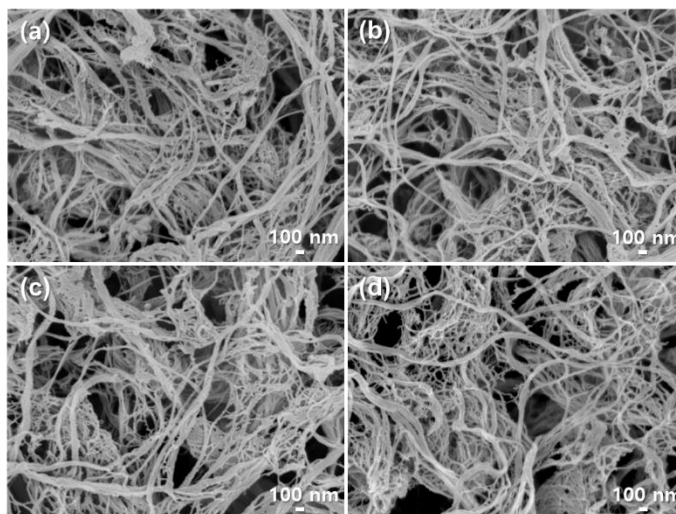


Fig. 5. FE-SEM images of NFCs manufactured from C-BSP at the pass number of seven by adding (a) 0%, (b) 10%, (c) 20%, and (d) 30% of GMA to the oven-dried NFC fibers

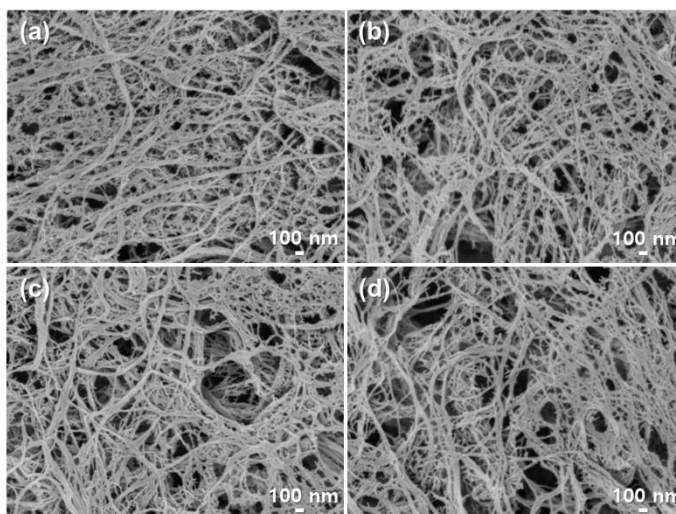


Fig. 6. FE-SEM images of NFCs manufactured from Hw-BKP at the pass number of seven by adding (a) 0%, (b) 10%, (c) 20%, and (d) 30% of GMA to the oven-dried NFC fibers

Figure 7 shows the low-shear viscosity of NFCs made from C-BSP and Hw-BKP depending on the added amount of GMA and the pass number of micro-grinding. When GMA (0%) was not added, the viscosity of anionic NFC slurry increased with the increase of pass number, and NFC from Hw-BKP showed higher viscosity than C-BSP at the same micro-grinding pass number. Saarikoski *et al.* (2012) and Grüneberger *et al.* (2014) reported that the low-shear viscosity of NFC was proportional to its nanofibril content and

specific surface. It was thought that the nanofibril content and specific surface area of NFC made from Hw-BKP were higher than those of one made from C-BSP at the same step of micro-grinding due to the smaller fiber size of Hw-BKP. However, as the amount of GMA increased, the viscosity of cationic NFC slurry did not change irrespectively of pulp type because the quaternization did not affect the fiber width of cationic NFC, confirmed by Figs. 4, 5, and 6. Therefore, it was confirmed that relatively higher mechanical energy was required to manufacture anionic NFC from C-BSP than Hw-BKP. The quaternization using GMA did not change the fiber width and low-shear viscosity of NFCs.

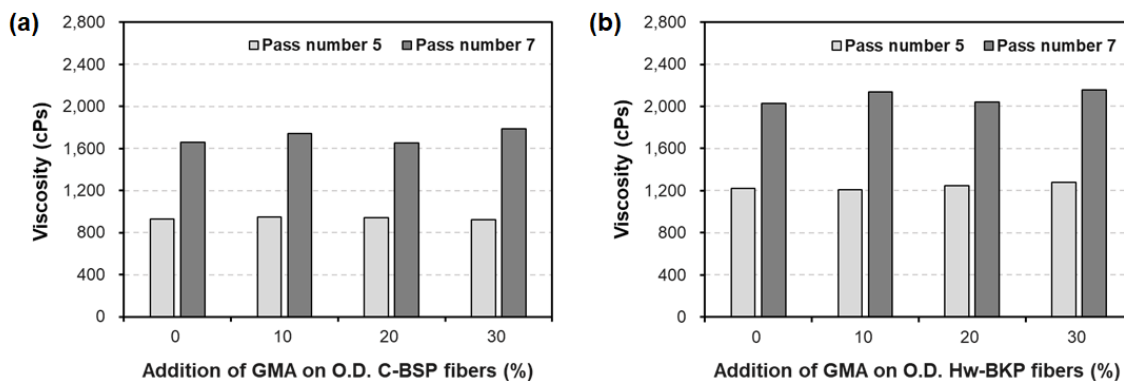


Fig. 7. Low-shear viscosity of NFCs made from (a) C-BSP and (b) Hw-BKP as a function of added GMA amount and the pass number of micro-grinding

Zeta Potential and FT-IR Analysis of NFCs

To identify the tertiary amines introduced on anionic NFC during the quaternization using GMA, FT-IR spectra were acquired for NFC pads fabricated from C-BSP, as shown in Fig. 8. Because the FT-IR peaks at 1,342 to 1,266 cm^{-1} represent the C–N group stretching vibrations, the peaks in this range should be observed as high-intensity bands (Gunasekaran and Sailatha 2009; Das *et al.* 2019). The anionic NFC made from C-BSP with the pass number of five did not show the peaks at 1,342 to 1,266 cm^{-1} , but the peaks in this range started to appear as GMA was introduced to anionic NFC, and the pass number was increased. Therefore, the quaternization using GMA effectively introduced tertiary amines on cationic NFC.

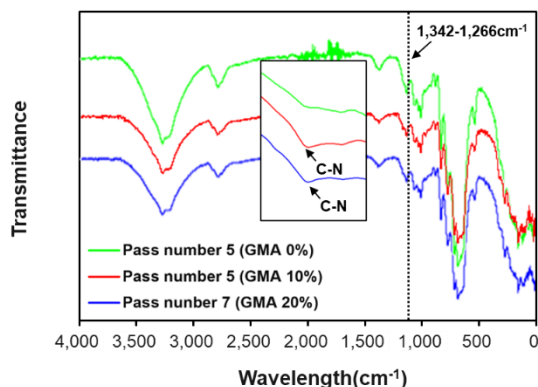


Fig. 8. FT-IR spectra of NFCs made from C-BSP depending on the amount of GMA added and the pass number of micro-grinding

Figure 9 shows the average zeta potential of NFCs prepared from C-BSP and Hw-BKP depending on the added amount of GMA and the pass number of micro-grinding. In C-BSP, the average zeta potential was reversed to a positive value when 10% of GMA was added. In Hw-BKP, the average zeta potential was reversed to a positive value when 20% of GMA was added. However, in both pulps, there was no difference in zeta potential due to the change in the pass number of micro-grinding. Figures 10 and 11 show the zeta potential distributions of NFCs manufactured from C-BSP and Hw-BKP, respectively, depending on the added amount of GMA and the pass number of micro-grinding. When 10% of GMA was added into anionic NFC prepared from C-BSP, all the fibrils were reversed from negative to positive for a pass number of five. However, when the pass number was seven, at least 20% of GMA was required to reverse the zeta potential of all fibrils in cationic NFC from C-BSP. However, for Hw-BKP, even 20% of GMA was insufficient to reverse the zeta potential of cationic NFC irrespective of the micro-grinding pass number. After the addition of 30% GMA, the zeta potential of cationic NFC was reversed for Hw-BKP.

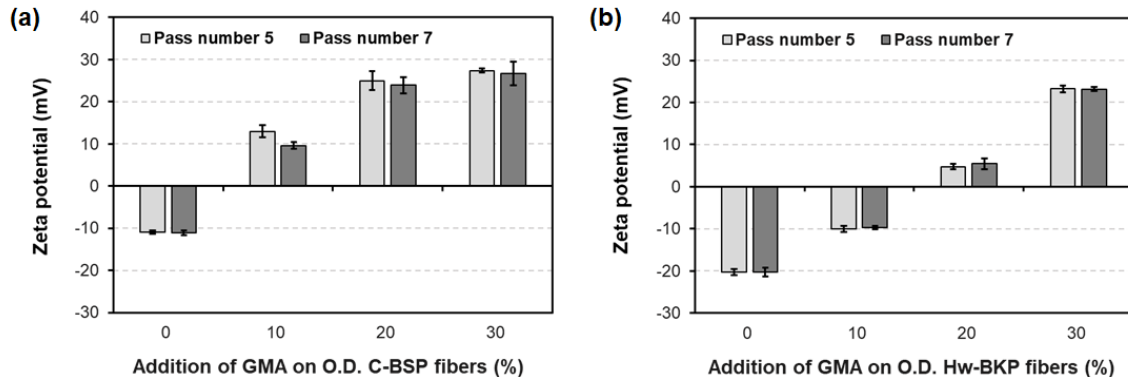


Fig. 9. Average zeta potential of NFCs manufactured from (a) C-BSP and (b) Hw-BKP depending on the amount of GMA added and the pass number of micro-grinding

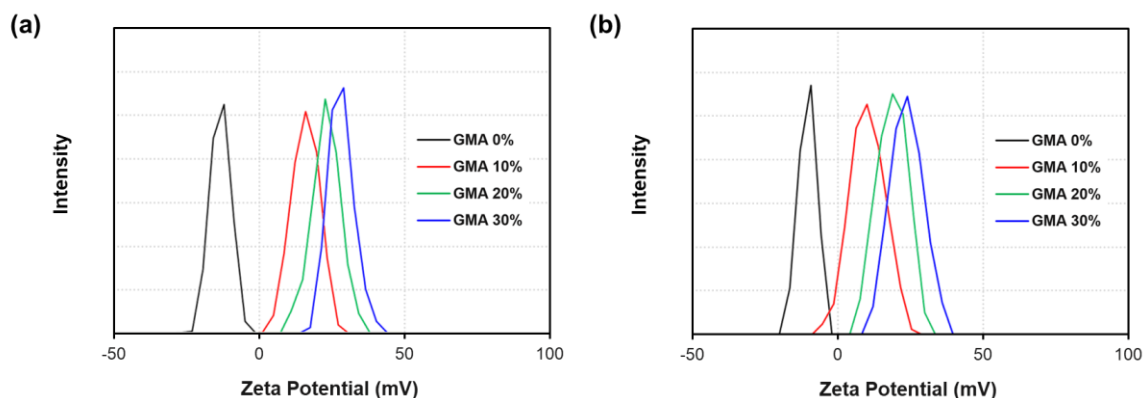


Fig. 10. Zeta potential distribution of NFCs made from C-BSP depending on the pass number of micro-grinding: (a) pass number 5 and (b) pass number 7

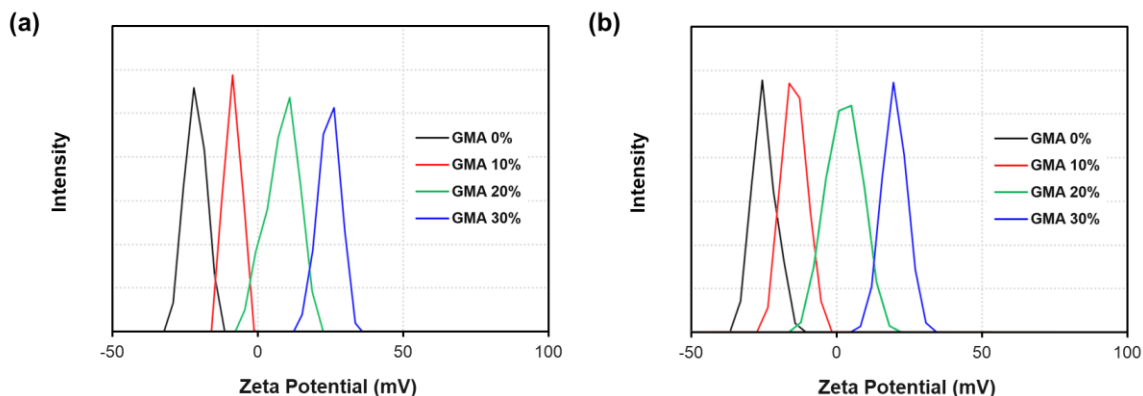


Fig. 11. Zeta-potential distribution of NFCs made from Hw-BKP depending on the pass number of micro-grinding: (a) pass number 5 and (b) pass number 7

The fiber width decreased, and the low-shear viscosity of cationic NFC increased as the nanofibril content increased (Saarikoski *et al.* 2012; Grüneberger *et al.* 2014; Lee *et al.* 2019). Because nanofibrils have a higher specific surface area than microfibrils, more GMA is required to electrostatically induce charge reversal in anionic NFC with higher nanofibril content (Grüneberger *et al.* 2014). Thus, anionic NFC made from C-BSP showed higher fiber width and lower viscosity than Hw-BKP; less GMA was required to prepare cationic NFC from anionic NFC using C-BSP. Therefore, it was concluded that cationic NFC could be manufactured *via* the quaternization of anionic NFC made from C-BSP using less GMA addition than that for Hw-BKP.

CONCLUSIONS

1. Anionic nano-fibrillated cellulose (NFC) was manufactured by beating and micro-grinding treatments of cotton-bleached soda pulp (C-BSP) and hardwood-bleached kraft pulp (Hw-BKP), respectively. After that, cationic NFC was manufactured *via* quaternization of anionic NFC using glycidyl trimethyl ammonium chloride (GMA).
2. Relatively higher mechanical energy was required to fabricate anionic NFC from C-BSP than that for Hw-BKP, and the amount of GMA used for quaternization did not impact the fiber width and viscosities of cationic NFCs. Quaternization using GMA as a post treatment electrostatically induced charge reversal in anionic NFC and was confirmed by Fourier transform infrared (FT-IR) and zeta potential analyses.
3. It was concluded that C-BSP could manufacture cationic NFC *via* quaternization of anionic NFC with less amount of GMA than Hw-BKP
4. Cationic NFC made from C-BSP can be widely used for manufacturing various products, which require the cationic electrostatic property and high low-shear viscosity including a strength enhancer and barrier coating agent in papermaking process, a thickener of the emulsions, and membrane filter for removing anions from the contaminated water.

ACKNOWLEDGMENTS

This work was supported by the National Research Foundation of Korea (NRF) grant funded by the Korea government (MSIT) (No. NRF-2022R1A2C1007565).

REFERENCES CITED

- Ashori, A., Babae, M., Jonoobi, M., and Hamzeh, Y. (2014). "Solvent-free acetylation of cellulose nanofibers for improving compatibility and dispersion," *Carbohydrate Polymers* 102, 369-375. DOI: 10.1016/j.carbpol.2013.11.067
- Aulin, C., Johansson, E., Wågberg, L., and Lindström, T. (2010). "Self-organized films from cellulose I nanofibrils using the layer-by-layer technique," *Biomacromolecules* 11(4), 872-882. DOI: 10.1021/bm100075e
- Balea, A., Fuente, E., Monte, M. C., Merayo, N., Campano, C., Negro, C., and Blanco, A. (2020). "Industrial application of nanocelluloses in papermaking: A review of challenges, technical solutions, and market perspectives," *Molecules* 25(3), 526. DOI: 10.3390/molecules25030526
- Bansal, M., Kumar, D., Chauhan, G. S., Kaushik, A., and Kaur, G. (2021). "Functionalization of nanocellulose to quaternized nanocellulose tri-iodide and its evaluation as an antimicrobial agent," *International Journal of Biological Macromolecules* 190, 1007-1014. DOI: 10.1016/j.ijbiomac.2021.08.228
- Beltramino, F., Roncero, M. B., Vidal, T., and Valls, C. (2018). "Facilitating the selection of raw materials: Evaluation of the effects of TCF and ECF bleaching sequences on different wood and non-wood pulps," *Afinidad* 75(582), 91-96.
- Candan, Z., Tozluoglu, A., Gonultas, O., Yildirim, M., Fidan, H., Alma, M. H., and Salan, T. (2022). "Nanocellulose: Sustainable biomaterial for developing novel adhesives and composites," *Industrial Applications of Nanocellulose and Its Nanocomposites*, pp. 49-137. DOI: 10.1016/B978-0-323-89909-3.00015-8
- Chaker, A., and Boufi, S. (2015). "Cationic nanofibrillar cellulose with high antibacterial properties," *Carbohydrate Polymers* 131, 224-232. DOI: 10.1016/j.carbpol.2015.06.003
- Charreau, H., Cavallo, E., and Foresti, M. L. (2020). "Patents involving nanocellulose: Analysis of their evolution since 2010," *Carbohydrate Polymers* 237, article ID 116039. DOI: 10.1016/j.carbpol.2020.116039
- Correia, J., Oliveira, F. R., Valle, R. D. C. S. C., and Valle, J. A. B. (2021). "Preparation of cationic cotton through reaction with different polyelectrolytes," *Cellulose* 28, 11679-11700. DOI: 10.1007/s10570-021-04260-4
- Das, G., Park, B. J., Kim, J. H., Kang, D. H., and Yoon, H. H. (2019). "Quaternized cellulose and graphene oxide crosslinked polyphenylene oxide based anion exchange membrane," *Scientific Reports* 9, article ID 9572. DOI: 10.1038/s41598-019-45947-w
- Deng, X., Ye, S., Wan, L., Wu, J., Sun, H., Ni, Y., and Liu, F. (2022). "Study on dissolution and modification of cotton fiber in different growth stages," *Materials* 15(7), article 2685. DOI: 10.3390/ma15072685
- Eichhorn, S. J., Dufresne, A., Aranguren, M., Marcovich, N. E., Capadona, J. R., Rowan, S. J., Weder, C., Thielemans, W., Roman, M., Renneckar, S., *et al.* (2010). "Review: Current international research into cellulose nanofibres and nanocomposites," *Journal*

- of Materials Science* 45, 1-33. DOI: 10.1007/s10853-009-3874-0
- Etale, A., Nhlane, D. S., Mosai, A. K., Mhlongo, J., Khan, A., Rumbold, K., and Nuapia, Y. B. (2021). "Synthesis and application of cationised cellulose for removal of Cr(VI) from acid mine-drainage contaminated water," *AAS Open Research* 4(4), 1-19. DOI: 10.12688/aasopenres.13182.1
- Grüneberger, F., Künniger, T., Zimmermann, T., and Martin, A. (2014). "Rheology of nanofibrillated cellulose/acrylate systems for coating applications," *Cellulose* 21, 1313-1326. DOI: 10.1007/s10570-014-0248-9
- Gunasekaran, S., and Sailatha, E. (2009). "Vibrational analysis of pyrazinamide," *Indian Journal of Pure and Applied Physics* 47, 259-264.
- Jo, H. M., Lee, Y. H., Kim, D. H., Lee, S. H., and Lee, J. Y. (2021). "Development of membrane filter for water treatment using anionic and cationic cellulose nanofibers," *Journal of Korea TAPPI* 53(6), 61-68. DOI: 10.7584/JKTAPPI.2021.12.53.6.61
- Jo, H. M., Kim, C. H., Lee, S. H., and Lee, J. Y. (2022). "Multi-layer barrier coating technology using nano-fibrillated cellulose and a hydrophobic coating agent," *BioResources* 17(4), 6222-6233. DOI: 10.15376/biores.17.4.6222-6233
- Korea Rural Economics Institute (2020). *Agriculture in Korea 2020*, Agriculture Industry Trends by Item, Korea Rural Economic Institute, Naju, Republic of Korea.
- KS M 7035 (2018). "Testing method for alcohol-benzene soluble matters in raw material for pulp," Korean Agency for Technology and Standards, Eumseong-gun, Chungcheongbuk-do, Republic of Korea.
- Lee, J. Y., Park, T. U., Kim, E. H., Jo, H. M., Kim, C. H., Kim, T. Y., Heo, Y. D., Lee, J. H., and Kim, J. K. (2017). "Effect of production conditions on the characteristics and the drainage of cellulose nano-fibrils," *Journal of Korea TAPPI* 49(3), 126-135. DOI: 10.7584/JKTAPPI.2017.06.49.3.126
- Lee, J. Y., Kim, K. M., Kim, S. H., Jo, H. M., and Kim, C. H. (2019). "Study on the quarternization reaction conditions for cationic cellulose nanofibril," *Journal of Korea TAPPI* 51(6), 144-151. DOI: 10.7584/JKTAPPI.2019.12.51.6.144
- Lee, J. Y., Jo, H. M., Lee, Y. H., and Lee, J. Y. (2021). "Effect of polyelectrolyte-cationized cellulose nanofibril on the properties of paper," *Journal of Korea TAPPI* 53(3), 49-56. DOI: 10.7584/JKTAPPI.2021.06.53.3.49
- Lee, S. H., Kim, D. H., Jo, H. M., and Lee, J. Y. (2022). "Characterization of paper mulberry bast fiber and cotton linter fiber for nanocellulose production," *Journal of Korea TAPPI* 54(5), 49-54. DOI: 10.7584/JKTAPPI.2022.10.54.5.49
- Li, J., Song, Z., Li, D., Shang, S., and Guo, Y. (2014). "Cotton cellulose nanofiber-reinforced high density polyethylene composites prepared with two different pretreatment methods," *Industrial Crops and Products* 59, 318-328. DOI: 10.1016/j.indcrop.2014.05.033
- Liimatainen, H., Suopajärvi, T., Sirviö, J., Hormib, O., and Niinimäki, J. (2014). "Fabrication of cationic cellulosic nanofibrils through aqueous quaternization pretreatment and their use in colloid aggregation," *Carbohydrate Polymers* 103, 187-192. DOI: 10.1016/j.carbpol.2013.12.042
- Morais, J. P. S., Rosa, M., Filho, M., Nascimento, L. D., Nascimento, D. M., and Cassales, A. R. (2013). "Extraction and characterization of nanocellulose structures from raw cotton linter," *Carbohydrate Polymers* 91, 229-235. DOI: 10.1016/j.carbpol.2012.08.010

- Naddeem, H., Athar, M., Dehghani, M., Garnier, G., and Warren, B. (2022). "Recent advancements, trends, fundamental challenges and opportunities in spray deposited cellulose nanofibril films for packaging applications," *Science of The Total Environment* 836, article 155654. DOI: 10.1016/j.scitotenv.2022.155654
- Nechyporchuk, O., Belgacem, M. N., and Bras, J. (2016). "Production of cellulose nanofibrils: A review of recent advances," *Industrial Crops and Products* 93, 2-25. DOI: 10.1016/j.indcrop.2016.02.016
- Norizan, M. N., Shazleen, S. S., Alias, A. H., Sabaruddin, F. A., Asyraf, M. R. M., Zainudin, E. S., Abdullah, N., Samsudin, M. S., Kamarudin, S. H., and Norrahim, M. N. F. (2022). "Nanocellulose-based nanocomposites for sustainable applications: A review," *Nanomaterials* 12(19), 3483. DOI: 10.3390/nano12193483
- Oh, Y. J., Park, S. Y., Yook, S. Y., Shin, H. N., Lee, H. L., and Youn, H. J. (2022). "A waterproof cellulose nanofibril sheet prepared by the deposition of an alkyl ketene dimer on a controlled porous structure," *Cellulose* 29, 6645-6657. DOI: 10.1007/s10570-022-04701-8
- Park, T. U., Lee, J. Y., Jo, H. M., and Kim, K. M. (2018). "Utilization of cellulose micro/nanofibrils as paper additive for the manufacturing of security paper," *BioResources* 13(4), 7780-7791. DOI: 10.15376/biores.13.4.7780-7791
- Park, Y. C., and Kim, G. J. (2010). "Cotton cellulose recycle fiber," *Fiber Technology and Industry* 14, 71-77.
- Pennells, J., Godwin, I. D., Amiralian, N., and Martin, D. J. (2020). "Trends in the production of cellulose nanofibers from non-wood sources," *Cellulose* 27(3), 575-593. DOI: 10.1007/s10570-019-02828-9
- Qin, C., Yao, M., Liu, Y., Yang, Y., Zong, Y., and Zhao, H. (2020). "MFC/NFC- based foam/aerogel for production of porous materials: Preparation, properties and applications," *Materials* 13(23), article ID 5568. DOI: 10.3390/ma13235568
- Ruiz-Caldas, M. X., Carlsson, J., Sadiktsis, L., Jaworski, A., Nilsson, U., and Mathew, A. P. (2022). "Cellulose nanocrystals from postconsumer cotton and blended fabrics: A study on their properties, chemical composition, and process efficiency," *ACS Sustainable Chemistry and Engineering* 10(11), 3787-3798. DOI: 10.1021/acssuschemeng.2c00797
- Saarikoski, E., Saarinen, T., Salmela, J., and Seppälä, J. (2012). "Flocculated flow of microfibrillated cellulose water suspensions: An imaging approach for characterization of rheological behaviour," *Cellulose* 19, 647-659. DOI: 10.1007/s10570-012-9661-0
- Sanchez-Salvador, J. L., Balea, A., Monte, M. C., Negro, C., Miller, M., Olson, J., and Blanco, A. (2020). "Comparison of mechanical and chemical nanocellulose as additives to reinforce recycled cardboard," *Scientific Reports* 10, article 3778. DOI: 10.1038/s41598-020-60507-3
- Sato, A., Kabusaki, D., Okumura, H., Nakatani, T., Nakatsubo, F., and Yano, H. (2016). "Surface modification of cellulose nanofibers with alkenyl succinic anhydride for high-density polyethylene reinforcement," *Composites Part A: Applied Science and Manufacturing* 83, 72-79. DOI: 10.1016/j.compositesa.2015.11.009
- Sczostak, A. (2009). "Cotton linters: An alternative cellulosic raw material," *Macromolecular Symposia* 280, 45-53. DOI: 10.1002/masy.200950606
- Sofi, S. A., Muzaffar, K., Farroq, A., Rafiq, S., Majid, D., Makroo, H. A., Mir, S. A., Khaneghah, A. M., Barba, F. J., and Dar, B. N. (2023). "Spectroscopic techniques for

- elucidation of structural changes in temperate cowpea cultivars under germination: A useful tool for quality determination and industrial application," *Applied Food Research* 3, article ID 100246. DOI: 10.1016/j.afres.2022.100246
- TAPPI T211 om-07 (2007). "Ash in wood, pulp, paper and paperboard: Combustion at 525 °C," TAPPI Press, Atlanta, GA, USA.
- Wise, L. E., Murphy, M., and D'adieco, A. A. (1946). "Chlorite holocellulose, its fractionation and bearing on summative wood analysis and on studies on the hemicelluloses," *Paper Trade Journal* 122(2), 35-43.
- Yasim-Anuar, T. A. T., Ariffin, H., Norrrahim, M. N. F., Hassan, M. A., Andou, Y., Tsukegi, T., and Nishida, H. (2020). "Well-dispersed cellulose nanofiber in low density polyethylene nanocomposite by liquid-assisted extrusion," *Polymers* 12(4), article 927. DOI:10.3390/polym12040927
- Yi, T., Zhao, H., Mo, Q., Pan, D., Liu, Y., Huang, L., Xu, H., Hu, B., and Song, H. (2020). "From cellulose to cellulose nanofibrils-A comprehensive review of the preparation and modification of cellulose nanofibrils," *Materials* 13(22), article 5062. DOI: 10.3390/ma13225062
- Zinge, C., and Kandasubramanian, B. (2020). "Nanocellulose based biodegradable polymers," *European Polymer Journal* 133, article ID 109758. DOI: 10.1016/j.eurpolymj.2020.109758

Article submitted: January 20, 2023; Peer review completed: February 11, 2023; Revised version received: February 27, 2023; Accepted: March 10, 2023; Published: March 21, 2023.

DOI: 10.15376/biores.18.2.3328-3341